Nuclear Magnetic Resonance Studies of a Series of Radical–Radical Dimerization Reactions

David J. Williams and Robert Kreilick

Contribution from the Department of Chemistry, University of Rochester, Rochester, New York 14627. *Received November 14, 1967*

Abstract: Nuclear magnetic resonance techniques have been used to study the dimerization of a series of 2,6-di-*t*-butyl-4-substituted phenoxy radicals. Rate constants for the dissociation of the dimer into two radicals and for rearrangement of the two halves of the dimer were determined. In some instances the reactions were studied in a series of solvents. Equilibrium constants for the dissociation reaction were measured by electron spin resonance spectroscopy. A mechanism is proposed in which the two reactions proceed through a common intermediate. Thermodynamic parameters are calculated for the various reactions.

In an earlier publication,[1] we reported an nmr study of the kinetics of a radical–radical dimerization reaction. The rate constant for dissociation of the diamagnetic dimer into two free radicals was determined from broadening of the dimer's nmr lines. A second reaction involving rearrangement of the two magnetically nonequivalent ends of the dimer was also detected. We have extended this type of study to a series of radical–radical dimerization reactions. A mechanism is proposed to explain the kinetic and thermodynamic data which were determined. The reactions which were studied are shown in eq 1.

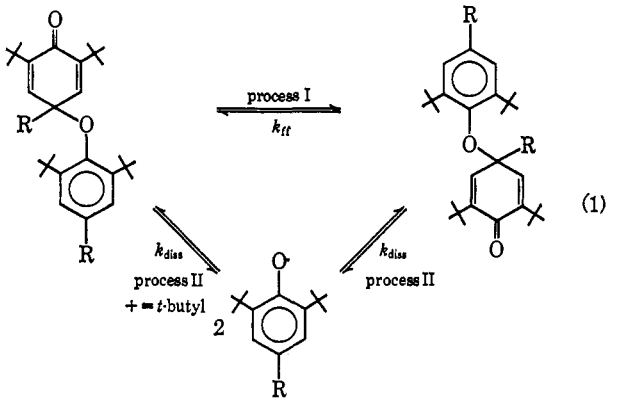

(1)

I, R = $COCH_3$ IV, R = $CO_2C_2H_5$
II, R = CO-*t*-C_4H_9 V, R = CO_2-*c*-C_6H_{11}
III, R = CO_2CH_3 VI, R = CN

The dissociation reaction (process II) interchanges the magnetic environment of the nuclei between diamagnetic and paramagnetic states. The contribution of such an exchange reaction to the breadth of a given nuclear resonance line is[2]

$$\left(\frac{1}{T_2}\right) = 1/t_D\left[\frac{(at/2)^2}{1 + (at/2)^2}\right] \qquad (2)$$

In this expression, t_D is the lifetime of the diamagnetic state, t is the lifetime of the paramagnetic state, and a is the electron-nuclei coupling constant for the group of nuclei whose line width is being measured. In the case where $(at/2)^2$ is much greater than 1, this equation reduces to

$$(1/T_2) = 1/t_D \qquad (3)$$

A sufficient condition for the applicability of eq 3 is that the electron spin resonance spectrum of the paramagnetic species exhibit hyperfine splitting from the group of nuclei whose line width is being measured. This condition was fulfilled in each of the cases studied.

The flip–flop reaction (process I) interchanges the magnetic environment of the nuclei between two different diamagnetic states. Equations relating line shapes to lifetimes, for reactions of this type, are well worked out.[3] The rate of the flip–flop reaction was faster than that of the dissociation reaction in each of the cases studied. In some cases, both reactions were slow enough to obtain well-resolved nmr spectra at low temperatures. Separate lines were observed from the protons on the aromatic and quinone rings and from the *t*-butyl protons on the two rings. The protons on the R groups connected to the two different rings were magnetically indistinguishable.

The flip–flop reaction interchanges the magnetic environment of the aromatic and quinone ring and *t*-butyl protons but does not affect protons on the R group. The chemical shift between the two types of *t*-butyl protons was small and these lines collapsed into a single, exchanged narrowed line over a relatively small temperature range. The chemical shift between the lines from the aromatic and quinone ring protons was larger. These lines broadened with increasing temperature, collapsed into a single line which began to narrow, and then broadened again. In some cases, the rate of process I was rapid, even at the lowest accessible temperatures, and single lines were observed for the ring and *t*-butyl protons. In these cases we were only able to set a lower limit on the rate constant for process I.

The nmr spectra of the three esters, at −60° in chloroform-*d*, are shown in Figure 1. The rate of process I is fast enough to collapse the ring proton lines of compounds III and IV into single lines. The rate is slower for compound V, and one observes separate lines from the aromatic and quinone ring protons. The characteristic temperature dependence of the nmr spectra has been shown previously for compound I in chloroform-*d*.[1]

(1) D. J. Williams and R. W. Kreilick, *J. Am. Chem. Soc.*, **89**, 3408 (1967).

(2) H. M. McConnell and S. B. Berger, *J. Chem. Phys.*, **27**, 230 (1957); C. S. Johnson, Jr., *ibid.*, **39**, 2111 (1963); R. W. Kreilick and S. I. Weissman, *J. Am. Chem. Soc.*, **88**, 2645 (1966).

(3) A. Allerhand, H. S. Gutowsky, J. Jones, and R. A. Meinzer, *ibid.*, **88**, 3185 (1966).

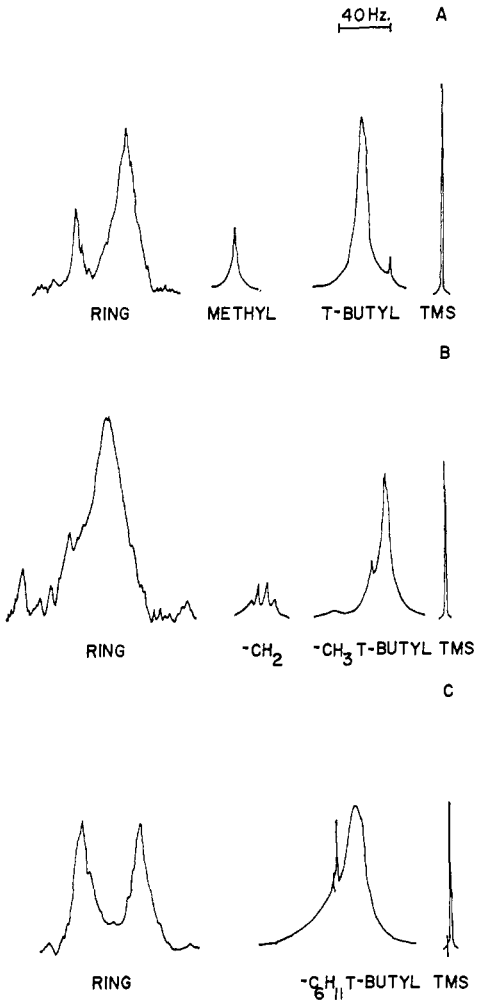

Figure 1. The nmr spectra of the three esters at −60° in chloroform-*d*: (A) compound III; (B) compound IV; (C) compound V.

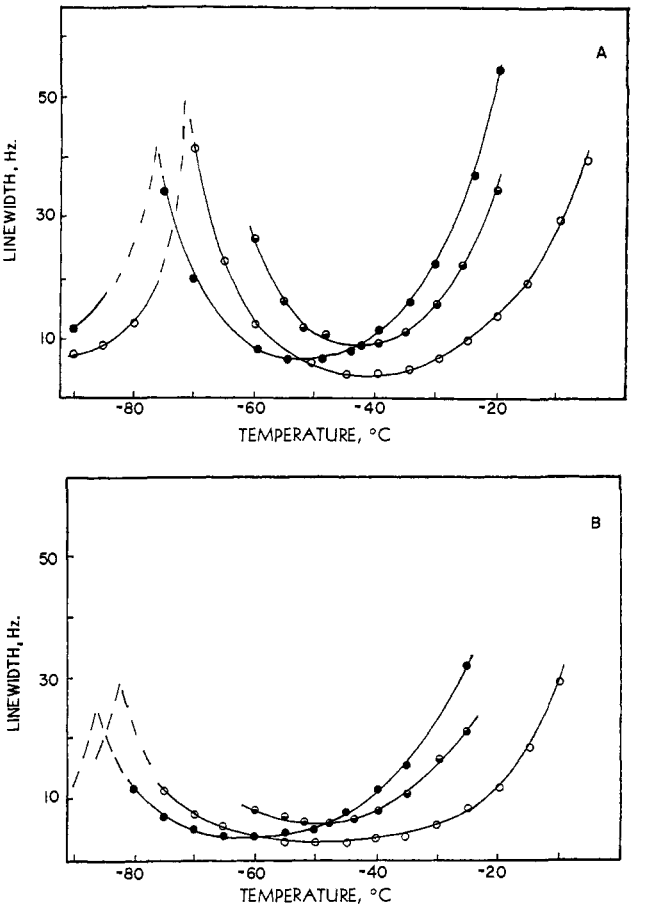

Figure 2. (A) Plot of the line width of the ring proton lines of compound IV *vs.* temperature. (B) Plot of the line width of the *t*-butyl proton lines of compound IV *vs.* temperature: ●, CS_2; ○, acetone-*d*; ◒, $CDCl_3$.

The line width of the peaks from the protons on the R group was determined by the rate of process II. When the rate of process I was rapid enough, and the ring or *t*-butyl lines had collapsed into a single exchange narrowed peak, the line widths of these signals were determined by the rate of process II. Information about the rate constant for the dissociation reaction could be obtained from the broadening of any of these lines. In general, the most intense peak, free of impurity lines, was used for the determination of k_{diss}. The rate of the dissociation reaction was slower than that of process I in all of the cases studied and did not contribute appreciably to the line width over the region in which process I was investigated.

Rate constants for compounds I and IV were determined with deuteriochloroform, deuterioacetone, and carbon disulfide as the solvent. The rate constants showed a marked solvent dependence. Figure 2 shows a plot of line width *vs.* temperature for compound IV in the various solvents. The rates were found to be fastest in chloroform and slowest in acetone.

The rates of reactions I and II should both show a first-order dependence on the dimer concentrations. The rate constants are related to lifetimes by

$$\begin{array}{cc} \text{process I} & \text{process II} \\ R_1 = k_{ff}[D] = [D]/t_{ff} & R_2 = k_{diss}[D] = [D]/t_{diss} \\ k_{ff} = 1/t_{ff} & k_{diss} = 1/t_{diss} \end{array} \quad (4)$$

where t_{ff} = dimer lifetime before exchange process I, and t_{diss} = dimer lifetime before exchange process II. Equation 4 predicts that the line broadening resulting from both of the exchange reactions should be independent of the dimer concentrations. In all of the cases studied the line broadening was found to be independent of concentration. Little or no broadening from dipole–dipole interactions with the free radical was observed because of the relatively low radical concentrations present.

The equilibrium constant for the dissociation reaction is given by

$$K = \frac{[\text{radical}]^2}{[\text{dimer}]} \quad (5)$$

We determined the equilibrium constant in each instance by measuring the free-radical concentration in solutions of known initial concentrations of dimer. Esr spectroscopy was used to determine the radical concentrations.

Experimental Section

A. Instruments. Nmr spectra were taken on a Varian A-60 nmr spectrometer. Esr measurements were made on a Jeolco 3BSX esr spectrometer. The temperature was varied by blowing cooled nitrogen gas over the samples.

B. Spectral Simulation. A Jeolco RA-1 digital computer was programmed with Gutowsky's equations for exchange between two diamagnetic sites.[4] Plots of the maximum to minimum ratio and

(4) H. S. Gutowsky and C. H. Holm, *J. Chem. Phys.*, **25**, 1228 (1956).

Table I. Chemical Shifts of the Various Dimers, τ Values

Compound	Solvent	*t*-Butyl	*R*	Quinone ring	Aromatic ring
I	$CDCl_3$	8.88 8.65	6.29	3.88	2.52
I	Acetone-*d*	8.89 8.66	6.65	3.65	2.51
I	CS_2	9.02 8.74	7.10	4.10	2.72
II	$CDCl_3$	8.92 8.65	8.83	4.01	2.55
III	$CDCl_3$	8.78[a]	6.11	3.17[a]	
IV	$CDCl_3$	8.79[a]	CH_3 8.12 (triplet)	3.16[a]	
			CH_2 5.71 (quartet)		
IV	Acetone-*d*	8.79[b]	CH_3 ...[c]	3.31	2.55
			CH_2 5.71 (quartet)		
IV	CS_2	8.90[b]	CH_3 ...[c]		
			CH_2 5.82 (quartet)	3.65	2.98
V	$CDCl_3$	8.78[a]	...[c]	3.46	2.72

[a] Exchange narrowed lines observed. [b] Center of incompletely resolved doublet. [c] Overlapped with *t*-butyl lines.

the line width of the exchange narrowed line *vs.* lifetime were made. These plots were used to determine t_{ff} from experimental values of either the maximum to minimum ratio or the line width.

C. Preparation of the Dimers. The dimers were made by oxidizing the appropriate phenol[5] with K_3FeCN_6 in aqueous alkaline methanol. The dimers precipitated out of solution as the reaction proceeded. The compounds were filtered and washed with water. The dimers were reasonably stable in the solid state but decomposed quickly in solutions in contact with the air. Except for compound III, all attempts to recrystallize the dimers were unsuccessful. In some cases the dimers prepared by this technique were not completely pure, and small impurity lines appeared in the nmr spectra. The values of the chemical shifts of the various dimers are given in Table I.

D. Equilibrium Constants. The equilibrium constants were determined by the method previously described.[1] Radical concentrations were determinated by measuring areas of the esr lines. The area was approximated by the intensity of the peak times its line width squared. In cases where esr lines are partially overlapped, this technique leads to some inaccuracy in the determination of the concentrations. In some instances the resolution of the esr spectra changed sufficiently with temperature to yield some scatter in our log K *vs.* $1/T$ plots and corresponding inaccuracies in our values for the standard enthalpy change. The equilibrium constant is larger for compound II than for the other dimers and there is a relatively small change in the radical concentration with temperature. As a consequence our values for K and $\Delta H°$ are somewhat inaccurate for this compound. Compound III in chloroform and compound IV in acetone also gave relatively poor numbers. Values of the equilibrium constants at the various temperatures were calculated with an IBM 7074 computer and a least-squares plot of log K *vs.* the reciprocal of temperature was made to determine standard enthalpy changes.

Results and Discussion

Kinetic data were determined for a series of compounds in an attempt to obtain information about steric and electronic influences on the rates of processes I and II. Compounds I and IV were also studied in a series of solvents to determine solvent effects. The rate of the flip–flop reaction was faster than that of the dissociation reaction in all of the cases studied. The rate constants for both reactions were larger for the series of esters than for the ketones. We were unable to observe the nmr spectrum of the nitrile (compound VI). Presumably, the rate of the dissociation reaction is fast enough to broaden the nmr lines into the base line. The rates of both reactions were observed to decrease as the steric bulk of the R group increased. The magnitude of the equilibrium constant increased with increased steric bulk.

(5) T. Matsuura, A. Nishinaga, and H. Cahnmann, *J. Org. Chem.*, **27**, 3620 (1962); R. W. Kreilick, *J. Am. Chem. Soc.*, **88**, 5284 (1966); E. Muller, A. Ricker, R. Mayer, and K. Scheffer, *Ann. Chem.*, **645**, 36 (1961).

Both reactions were studied over as wide a temperature range as possible, and activation enthalpies were calculated. The standard enthalpy change for the dissociation reaction was determined from the temperature dependence of the equilibrium constant. Representative plots of the log of the equilibrium constant *vs.* the reciprocal of temperature are given in Figure 3.

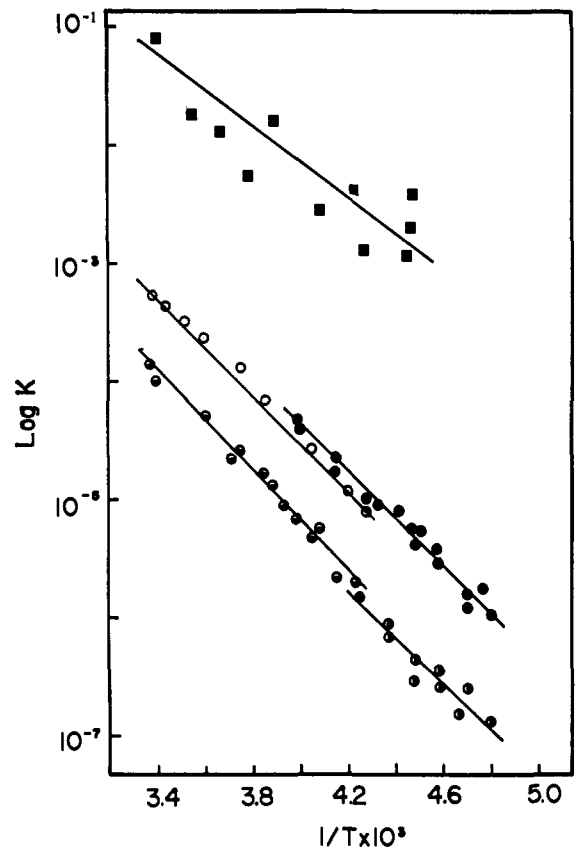

Figure 3. Plots of the log of the equilibrium constants *vs.* the reciprocal of temperature: ■, compound II in $CHCl_3$; ○, compound I in $CHCl_3$; ◒, compound I in CS_2; ●, compound IV in $CHCl_3$; ◑, compound IV in acetone.

The points are somewhat scattered for compound II in chloroform and compound IV in acetone because of experimental difficulties. This scatter is reflected in our values for the standard enthalpy change. The equilibrium was found to shift more toward the side of the dissociated product as the bulk of the R group

Table II. Rate and Equilibrium Data at 250°K

Compound	Solvent	k_1	k_{diss}	$k_4 \times 10^{-5}$	k_2/k_3	$K \times 10^5$
I	$CDCl_3$	$(6.8 \pm 0.2) \times 10^2$	14 ± 1	7.7 ± 1	25	3.6 ± 1.0
I	Acetone-*d*	$(2.5 \pm 0.1) \times 10^2$	3.5 ± 0.5	7.0 ± 1	36	1.0 ± 0.2
I	CS_2	$(2.7 \pm 0.1) \times 10^2$	11 ± 1	30 ± 10	12	0.7 ± 0.2
II	$CDCl_3$	$(0.3 \pm 0.1) \times 10^2$	Slow[a]	...	...	500 ± 100
III	$CDCl_3$	$>10^5$ [b]	$(2.1 \pm 0.1) \times 10^2$	50 ± 10	...	8.5 ± 1.5
IV	$CDCl_3$	$>10^5$ [b]	$(1.9 \pm 0.1) \times 10^2$	77 ± 10	...	4.8 ± 1.0
IV	Acetone-*d*	$(8.0 \pm 0.2) \times 10^3$	35 ± 3	67 ± 10	116	1.0 ± 0.5
IV	CS_2	$(3.9 \pm 0.2) \times 10^4$	$(1.2 \pm 0.1) \times 10^2$	133 ± 10	160	1.9 ± 0.5
V	$CDCl_3$	$(1.0 \pm 0.1) \times 10^3$	15.0 ± 2	0.7 ± 0.1	33	43 ± 10
VI	$CDCl_3$	$>10^5$	...	...	...	70 ± 10

[a] No line broadening was observed from this reaction. [b] Exchange narrowed lines were observed at the lowest accessible temperature.

Table III. Thermodynamic Data at 250°K[a]

Compound	Solvent	$\Delta H°$	$\Delta H_1^{\ddagger}$	$\Delta H_{diss}^{\ddagger}$	$\Delta H_4^{\ddagger}$	$\Delta S°$	$\Delta S_1^{\ddagger}$	$\Delta S_{diss}^{\ddagger}$	$\Delta S_4^{\ddagger}$	$\Delta G°$	$\Delta G_1^{\ddagger}$	$\Delta G_{diss}^{\ddagger}$	$\Delta G_4^{\ddagger}$
I	$CDCl_3$	9.1	9.1	9.1	<1.0	16.1	−7.5	−14.0	−30	5.0	11.0	12.6	7.5
I	Acetone-*d*	11.6	6.6	7.0	−4.6	23.4	−19.5	−25.1	−48.5	5.7	11.5	13.3	7.6
I	CS_2	10.3	7.2	6.8	−3.5	17.6	−17.0	−23.7	−41.3	5.9	11.4	12.7	6.8
II	$CDCl_3$	6.9	2.9	...	...	17.1	−38.5	...	...	2.6	12.5	...	...
III	$CDCl_3$	11.6	...	10.0	−1.6	27.7	...	−5.1	−32.7	4.7	...	11.3	6.6
IV	$CDCl_3$	8.8	...	8.5	−0.4	15.5	...	−11.4	−26.9	4.9	...	11.3	6.4
IV	Acetone-*d*	12.0	8.2	9.2	−2.8	25.1	−6.5	−11.7	−36.8	5.7	9.8	12.1	6.4
IV	CS_2	10.9	7.1	8.1	−2.8	21.9	−7.5	−13.8	−35.6	5.4	9.0	11.5	6.1
V	$CDCl_3$	7.2	7.8	9.0	1.8	13.3	−12.1	−14.3	−27.6	3.9	10.8	12.6	8.7
VI	$CDCl_3$	6.1	...	...	...	9.3	...	...	...	3.9	...	...	...

[a] Enthalpies and free energies are in kilocalories/mole. The estimated error is ±0.5 kcal/mole. Entropies are in entropy units. The estimated error is ± 2 eu.

increased. The magnitude of the standard enthalpy change decreased with increased size of the R group. Values for equilibrium constants and the standard enthalpy changes are given in Tables II and III.

Plots of the log of the rate constants *vs.* the reciprocal of temperature are given in Figures 4 and 5. The data from the rate measurements were more accurate than those from the equilibrium measurements. The activation enthalpies are therefore more reliable than the standard enthalpy changes. The magnitudes of the activation enthalpies for the two reactions were almost identical for all of the cases studied. The rate constants and activation enthalpies were found to decrease as the steric bulk of the R group increased. In the two cases studied, both the rate constants and the activation enthalpies showed a solvent dependence.

The same carbon–oxygen bond is broken in both the dissociation reaction and the flip–flop reaction. The resulting pair of free radicals must have a short lifetime (*ca.* 10^{-7} sec) or a contribution to the nmr line widths would be observed whenever this species was formed. A mechanism for the reactions observed can be written in which the two reactions proceed through the same short-lived intermediate. After the intermediate is formed, the radical pair could recombine to form either the starting material or the rearranged product, or the radicals could diffuse apart. The solvent dependence of the reactions could be explained by different types of solvation for this intermediate. The reaction can be written as shown in eq 6.

A second mechanism could be postulated in which the flip–flop reaction proceeded through an intermediate in which the new carbon–oxygen bond was formed as the original bond was broken. This type of mechanism would have rigid steric requirements for the highly hindered systems which were studied. As the activation enthalpies were almost identical for the two reactions, the relative rate constants were determined by entropy factors. It seems unlikely that the rate of the flip–flop reaction proceeding through a highly organized intermediate should be greater than that of the dissociation reaction. The observed similarity of the solvent dependence of the two reactions also leads us to favor a mechanism involving a common intermediate.

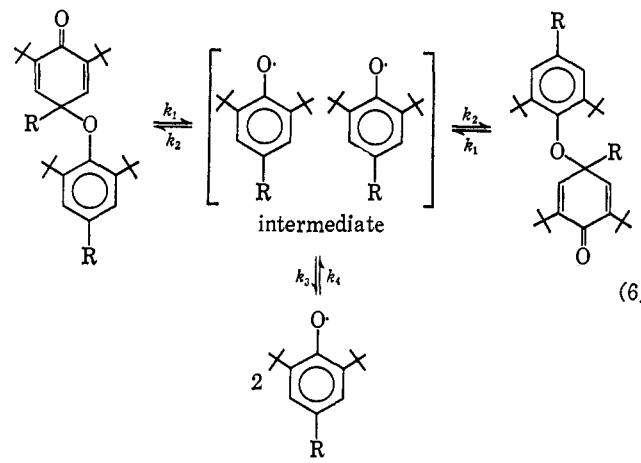

If one adopts this type of mechanism and assumes that the probabilities for recombination to make either form of the dimer are equal, the rate constant for the flip–flop reaction can be equated to $k_1/2$, and k_{diss} can be equated to $k_1k_3/2k_2$. Rate constants k_3 and k_2 refer to diffusion of the radical pair apart and to the radical–radical recombination reaction, respectively. The ratio of these two rate constants can be evaluated from the ratio of k_{ff} to k_{diss}. The rate constant for association of two radicals to form the intermediate (k_4) can be determined from the equilibrium constants,

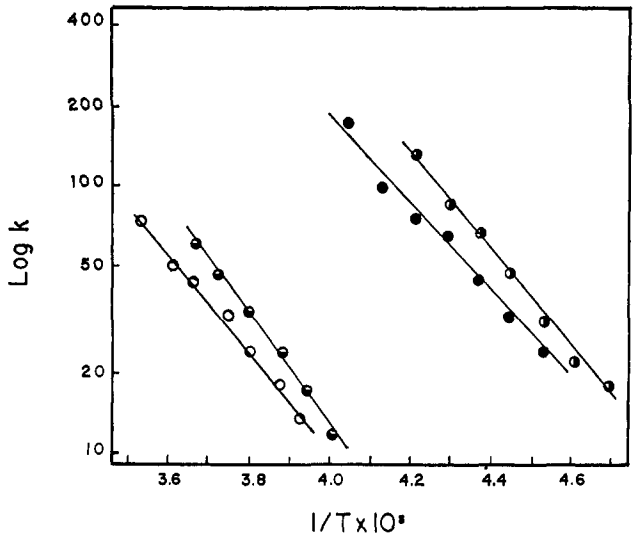

Figure 4. Plot of the log of rate constants *vs.* the reciprocal of temperature: ○, k_{diss} of compound I in CS_2; ◒, k_{diss} of compound I in $CDCl_3$; ●, k_{ff} of compound I in CS_2; ◑, k_{ff} of compound I in $CDCl_3$.

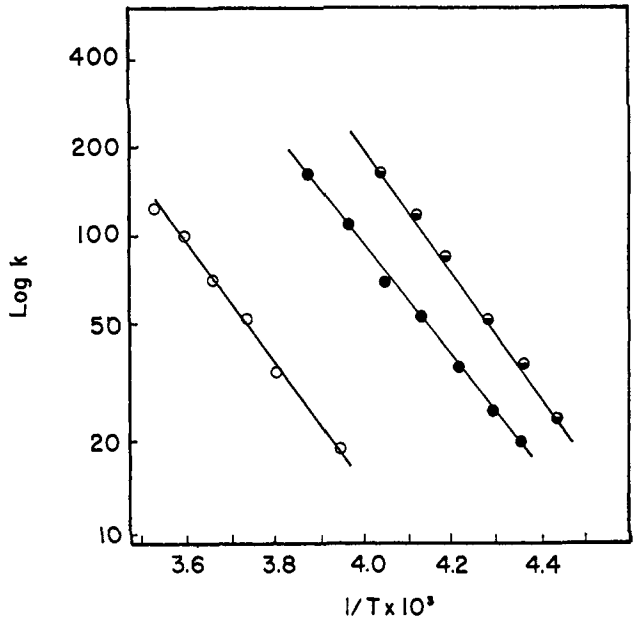

Figure 5. Plot of the log of rate constants *vs.* the reciprocal of temperature: ○, k_{diss} of compound V in $CDCl_3$; ●, k_{diss} of compound IV in $CDCl_3$; ◒, k_{diss} of compound III in $CDCl_3$.

(k_1k_3/k_2k_4) and k_{diss}. Values for the various rate constants at 250°K are given in Table II. In some cases, we had to extrapolate our plots of the temperature dependence of the rate constants in order to obtain values at 250°K. This technique produces a small error in some of the rate constants. The ratio of k_2 to k_3 showed a significant solvent dependence. The change in this ratio with solvent is probably due to changes in solvation of the radical pair intermediate.

We employed the absolute reaction rate theory in order to determine the activation free energies. A value of 0.5 was assumed for κ. The standard free-energy changes for the dissociation reactions ($\Delta G°$) were calculated from the equilibrium constants. Errors inherent in our determinations of the equilibrium constants are reflected in these values. Activation entropies and the standard entropy change for the dissociation reaction ($\Delta S°$) were determined from the free energies and enthalpies. These thermodynamic data are given in Table III.

Activation parameters for two radicals and the dimer going to the intermediate are obtained directly form the k_4's and k_1's. The rate constant for the dissociation reaction is a product of k_1, k_3, and $1/k_2$, and the activation terms determined are a sum of terms from the individual reactions. For example, the activation energy for dissociation is given by

$$\Delta H_{diss}^{\ddagger} = \Delta H_1^{\ddagger} + \Delta H_3^{\ddagger} - \Delta H_2^{\ddagger} \qquad (7)$$

The values of $\Delta H_{diss}^{\ddagger}$ and $\Delta H_1^{\ddagger}$ were very close to one another in all of the cases studied, implying that $\Delta H_2^{\ddagger}$ must nearly be equal to $\Delta H_3^{\ddagger}$. A negative value for the activation enthalpy of the radical–radical association reaction ($\Delta H_4^{\ddagger}$) was found in some cases.

Large entropy terms were found for each of the reactions, and these appear to be the dominant factors in the reaction scheme. The entropy factors probably reflect the ordering necessary for the reactions to proceed. The entropy change for the dissociation reactions (ΔS_{diss}) is more negative than $\Delta S_1^{\ddagger}$ in each case, showing

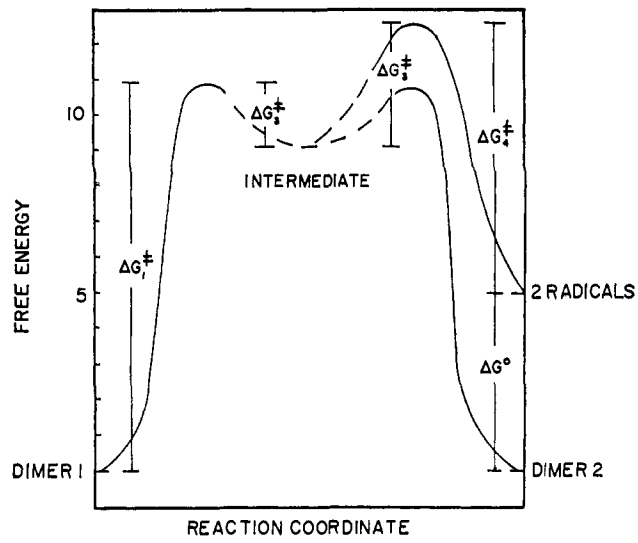

Figure 6. Plot of the free-energy change *vs.* reaction coordinate for compound I in chloroform. The depth of the well for the intermediate is uncertain and is depicted by dashed lines.

differences in $\Delta S_3^{\ddagger}$ and $\Delta S_2^{\ddagger}$. The variation in the entropy terms with solvent are probably due to changes in the ordering of the solvent molecules. The entropy term for the association reaction ($\Delta S_4^{\ddagger}$) is negative enough in each case to make the free-energy change ($\Delta G_4^{\ddagger}$) positive. A plot of free energy *vs.* the reaction coordinate is given in Figure 6.

It is difficult to sort out electronic and steric terms influencing these reactions. The esters studied had larger rate constants then the ketones in all instances. This effect may be due to changes in steric hindrance near the reaction site rather than an electronic effect. Increased steric bulk near the reaction site was observed to slow the reaction in all cases.

Conclusions

A series of radical–radical dimerization reactions have been studied using nuclear magnetic resonance techniques. Two different reactions, involving rearrangement of the dimer and dissociation of the dimer, were observed. A mechanism involving a common intermediate for the two reactions was proposed. Rate and thermodynamic data were determined for a series of different dimers. Solvent effects were also studied. The dominant factor in these reactions appeared to be the steric hindrance of groups substituted near the reaction site.

The Crystal Structure of the Bicyclic Phosphate $OP(OCH_2)_3CCH_3$[1a]

D. M. Nimrod, D. R. Fitzwater, and J. G. Verkade[1b]

Contribution from the Institute for Atomic Research and Department of Chemistry, Iowa State University, Ames, Iowa. *Received August 28, 1967*

Abstract: The structure of 1-oxo-4-methyl-2,6,7-trioxa-1-phosphabicyclo[2.2.2]octane, $OP(OCH_2)_3CCH_3$, has been determined by three-dimensional Fourier synthesis and full-matrix least-squares refinement of X-ray diffraction counter data. The crystals are orthorhombic, space group $Pmc2_1$, with unit cell dimensions $a = 6.74$ Å, $b = 5.96$ Å, $c = 17.77$ Å, four molecules per unit cell ($\rho_{calcd} = 1.53$, $\rho_{obsd} = 1.51$ g/cm^3). The data reveal that some strain is probably present in the bicyclic structure. The bonding of the oxygens to the phosphorus appears to be similar to that found in other trialkyl phosphates whose structures are known. The terminal O=P bond distance is 1.46 ± 0.02 Å, and the bridging P–O distances average 1.57 ± 0.02 Å. The O=P—O angle is 115.0 ± 1.1° and the O—P—O angle is 103.7 ± 0.6°. The O=P stretching frequency is compared with similar modes in open-chain phosphates and correlated qualitatively with the basicity of the oxygen.

Bicyclic alkoxy phosphites of the type $P(OCH_2)_3CR$ (where R = CH_3, C_2H_5, and n-C_5H_{11}) have been shown to function as strong ligands in the presence of transition metal ions,[2] transition metal carbonyls,[3] and boron-containing Lewis acids.[4] Although the general bicyclic structure of $P(OCH_2)_3CCH_3$ and $OP(OCH_2)_3CCH_3$ was deduced from their H^1 and P^{31} nmr spectra,[5] it was of interest to determine an accurate structure of $OP(OCH_2)_3CCH_3$ for several reasons. In addition to the fact that this study represents the first structural analysis of a bicyclic phosphate, the geometry of this molecule should closely approximate that of coordinated $P(OCH_2)_3CCH_3$ in transition metal complexes and adducts. Moreover, it should have structural parameters similar to that of stable phosphonium cations of the type $[RP(OCH_2)_3CCH_3]^+$,[6] as well as the phosphonium intermediates in the Michaelis–Arbuzov reactions of $P(OCH_2)_3CCH_3$.[7] It was also of interest to determine whether any of the structural features could account for the lack of extraction properties of the analogous $OP(OCH_2)_3C(CH_3)_4CH_3$ and the abnormally high O=P stretching frequency in compounds of the type $OP(OCH_2)_3CR$.[8]

(1) (a) This work was performed in the Ames Laboratory of the U. S. Atomic Energy Commission. Contribution No. 2125. (b) Author to whom inquiries should be addressed at the Department of Chemistry, Iowa State University, Ames, Iowa.

(2) K. J. Coskran, T. J. Huttemann, and J. G. Verkade, Advances in Chemistry Series, No. 62, American Chemical Society, Washington, D. C., 1967, p 590.

(3) D. G. Hendricker, R. E. McCarley, R. W. King, and J. G. Verkade, *Inorg. Chem.*, **5**, 639 (1966).

(4) J. G. Verkade, R. W. King, and C. W. Heitsch, *ibid.*, 3, 884 (1964).

(5) J. G. Verkade and R. W. King, *ibid.*, 1, 948 (1962).

(6) J. G. Verkade, T. J. Huttemann, M. K. Fung, and R. W. King, *ibid.*, 4, 83 (1965).

(7) R. D. Bertrand, G. K. McEwen, E. J. Boros, and J. G. Verkade, submitted for publication.

Experimental Section

Preparation. The preparation of $OP(OCH_2)_3CCH_3$ has been described elsewhere.[6] Crystals suitable for X-ray analysis were obtained by slow sublimation at 100° inside a water-cooled sublimation apparatus. The resulting long, needle-like, soft crystals were severed with a razor blade into near cubes. Torsional distortion of the resulting crystal was checked by examining Weissenberg photographs for drawn-out spots along the axis of rotation. A good single crystal for the collection of intensity data was obtained by this method, but later attempts to obtain suitable fresh crystals for the purpose of obtaining accurate lattice constants and for retaking part of the intensity data were not successful.

Crystal Data. Weissenberg and precession photographs with Cu Kα radiation revealed mmm Laue symmetry (orthorhombic). Observed systematic extinctions ($h0l$, $l \neq 2n$) were compatible with space groups Pmcm, P2cm, and $Pmc2_1$. The lattice parameters were calculated from precession and Weissenberg photographs using Cu Kα radiation and from measurements using a General Electric single-crystal orienter with Mo Kα and Cr Kα radiation. A least-squares lattice constant refinement program of Williams[9] was employed to obtain the following values and estimated standard deviations: $a = 6.736$ (0.003) Å, $b = 5.96$ (0.017) Å, $c = 17.768$ (0.004) Å. The calculated density for four molecules per unit cell, 1.53 g/cm^3, agrees favorably with the observed value of 1.51 g/cm^3 obtained by the flotation method in a mixture of benzene and carbon tetrachloride. On the basis of observed systematic extinctions not required by the space group symmetry along the a axis, together with a moderately well-grounded knowledge of the molecular structure, the Pmcm and P2cm space groups were eliminated as possibilities. (Elimination of Pmcm assumes that there is no disorder.)

Space requirements for the packing of the molecules also suggest the $Pmc2_1$ space group. Four molecules can be arranged in this space group and can account for the extra systematic extinction by placing a molecule on the $x = 0$ mirror and a crystallographically independent one on the $x = 1/2$ mirror.

Collection and Treatment of Data. A full octant of three-dimensional X-ray diffraction intensity data was gathered at room

(8) S. G. Goodman and J. G. Verkade, *Inorg. Chem.*, **5**, 498 (1966).

(9) D. E. Williams, USAEC Report, IS-1052, Ames Laboratory, Ames, Iowa.